Kinematic Analysis of the Multi-Link Five-Point Suspension System in Point Coordinates

Hazem Ali Attia*
Department of Mathematics, College of Science, King Saud University (Al-Qasseem Branch), P.O. Box 237, Buraidah 81999, KSA

In this paper, a numerical algorithm for the kinematic analysis of a multi-link five-point suspension system is presented. The kinematic analysis is carried out in terms of the rectangular Cartesian coordinates of some defined points in the links and at the joints. Geometric constraints are introduced to fix the relative positions between the points belonging to the same rigid body. Position, velocity and acceleration analyses are carried out. The presented formulation in terms of this system of coordinates is simple and involves only elementary mathematics. The results of the kinematic analysis are presented and discussed.

Key Words: Kinematic Analysis, Suspension Systems, Five-Point Suspension, Point Coordinates

1. Introduction

In recent years various methods for the kinematic analysis of spatial mechanisms have been developed. The different methods can be classified according to the type of coordinates chosen to determine their configuration and specify their constraints. Some formulations use a large set of absolute coordinates (Wehage and Haug, 1982; Nikravesh, 1988). The position and orientation of the rigid links in the mechanism are described with respect to the global reference coordinate system. The algebraic equations of constraints are introduced to represent the kinematic joints that connect the rigid bodies. Although in this type of formulation the constraint equations are easy to construct, it has the disadvantage of the large number of defined coordinates. Other formulations use sets of relative coordinates (Denavit and Hartenberg, 1955; Paul and Krajcinovic, 1970). The position of each link is defined with respect to the previous link by means of relative joint coordinates that depend on the type of the joint used. This type of formulation yields the constraints as a minimal set of algebraic equations. The constraint equations are derived based on loop closure equations and the resulting constraint equations are highly nonlinear and contain complex circular functions.

Another formulation which is based on point coordinates is discussed in (Garcia de Jalon et al., 1981, 1982; Vilallong et al., 1984; Akhras and Angeles, 1990; Attia, 1993). The configuration of the system is described in terms of the rectangular Cartesian coordinates of some defined points in the links and at the joints. The system constraint equations are then written to fix the relative positions of the points in each rigid link and also the relative positions between the different links determined by the type of joints connecting them.

In this paper the kinematic analysis of the multi-link five-point suspension system is carried out in terms of point coordinates. The position, velocity, and acceleration analyses are carried out to determine the positions, velocities, and accelerations for the unknown points and links in the mechanism. The velocities and accelerations of

* **E-mail**: ah1113@yahoo.com
TEL: +966-6-3800319; **FAX**: +966-6-3800911
Department of Mathematics, College of Science, King Saud University (Al-Qasseem Branch), P.O. Box 237, Buraidah 81999, KSA. (Manuscript **Received** October 30, 2002; **Revised** May 6, 2003)

other points of interest can also be calculated. The angular velocity and acceleration of any link in the mechanism are evaluated in terms of the Cartesian coordinates, velocities, and accelerations of the assigned points.

2. Modelling of the Multi-Link Five-Point Suspension System

The multi-link five-point suspension system is usually used for rear driven axles of current productions of Mercedes-Benz cars, Mazda 929, some BMW and Toyota Supra cars. The mechanical system consists of the main chassis, a multi-link five-point suspension mechanism, and the wheel as shown in Fig. 1. The system has three degrees of freedom (DOF). The chassis, since it is constrained to move vertically upward or downward, only one DOF out of its six DOF remains. The wheel has one-DOF corresponding to the rolling motion. Since the suspension mechanism connects the driven wheel to the chassis (specifically to the axle carrier) by rubber mountings, it can be simulated as five binary links connecting the chassis and the wheel knuckle through spherical joints at both ends of each link. Thus, the suspension mechanism consists of five links and ten spherical joints, and has only one-DOF (see Fig. 1).

2.1 Displacement analysis

The configuration of the mechanism can be specified by defining a set of points on the links and at the joints. Figure 2 presents the mechanism

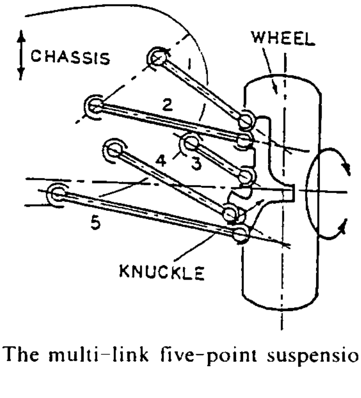

Fig. 1 The multi-link five-point suspension system

with the assigned points. Each binary link is replaced by two points located at the centre of the spherical joints at both ends, while the adjacent links are sharing common points. The whole mechanism is then replaced by ten points. Points 1, ⋯, 5 that are located at the chassis, are known points. The Cartesian coordinates of the unknown points 6, ⋯, 10 located on the knuckle define the motion variables. Therefore, 15 constraint equations are needed to solve for the 15 unknown Cartesian coordinates. The initial positions, velocities, and accelerations of points 1, ⋯, 5 are known from the driver data.

The constraints are either geometric or kinematic constraints. Geometric constraints are distance constraints that fix the relative positions of the points on a rigid link of the mechanism. The geometric constraint equations are expressed in the Cartesian coordinates of the points as follows,

$$(x_6-x_1)^2+(y_6-y_1)^2+(z_6-z_1)^2-d_{6,1}^2=0 \quad (1.1)$$

$$(x_7-x_2)^2+(y_7-y_2)^2+(z_7-z_2)^2-d_{7,2}^2=0 \quad (1.2)$$

$$(x_8-x_3)^2+(y_8-y_3)^2+(z_8-z_3)^2-d_{8,3}^2=0 \quad (1.3)$$

$$(x_9-x_4)^2+(y_9-y_4)^2+(z_9-z_4)^2-d_{9,4}^2=0 \quad (1.4)$$

$$(x_{10}-x_5)^2+(y_{10}-y_5)^2+(z_{10}-z_5)^2-d_{10,5}^2=0 \quad (1.5)$$

$$(x_7-x_6)^2+(y_7-y_6)^2+(z_7-z_6)^2-d_{7,6}^2=0 \quad (1.6)$$

$$(x_8-x_6)^2+(y_8-y_6)^2+(z_8-z_6)^2-d_{8,6}^2=0 \quad (1.7)$$

$$(x_9-x_6)^2+(y_9-y_6)^2+(z_9-z_6)^2-d_{9,6}^2=0 \quad (1.8)$$

$$(x_{10}-x_6)^2+(y_{10}-y_6)^2+(z_{10}-z_6)^2-d_{10,6}^2=0 \quad (1.9)$$

$$(x_8-x_7)^2+(y_8-y_7)^2+(z_8-z_7)^2-d_{8,7}^2=0 \quad (1.10)$$

$$(x_9-x_7)^2+(y_9-y_7)^2+(z_9-z_7)^2-d_{9,7}^2=0 \quad (1.11)$$

$$(x_{10}-x_7)^2+(y_{10}-y_7)^2+(z_{10}-z_7)^2-d_{10,7}^2=0 \quad (1.12)$$

$$(x_9-x_8)^2+(y_9-y_8)^2+(z_9-z_8)^2-d_{9,8}^2=0 \quad (1.13)$$

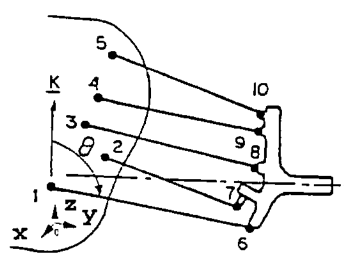

Fig. 2 The multi-link five-point suspension with the assigned points

$$(x_{10}-x_8)^2+(y_{10}-y_8)^2+(z_{10}-z_8)^2-d_{10,8}^2=0 \quad (1.14)$$

where $d_{i,j}$ is the distance between points i and j belonging to the same rigid link, and x_i, y_i, and z_i are the Cartesian coordinates of point i. Kinematic constraints result from the conditions imposed by the kinematic joints on the relative motion between the bodies they comprise. Points located at the centre of a spherical joint or at the axis of a revolute joint automatically eliminate all the kinematic constraints due to these joints. Moreover, driving constraints are added to the above constraints as functions of the input driving angular position θ (see Fig. 2) in the form,

$$(z_6-z_1)-d_{6,1}\cos(\theta)=0 \quad (1.15)$$

Equation (1) expresses the required 15 independent constraint equations in terms of the Cartesian coordinates of the assigned points. Given the set of the known coordinates of points 1, ⋯, 5 and the driving variable * at each instant, the nonlinear Eq. (1) can be solved by any iterative numerical method (Molian, 1968) to determine the 15 unknown Cartesian coordinates of points 6, ⋯, 10.

It should be noted that in this formulation, the kinematic constraints due to some common types of kinematic joints (e.g. revolute or spherical joints) can be automatically eliminated by properly locating the assigned points. The remaining kinematic constraints along with the geometric constraints are, in general, either linear or quadratic in the Cartesian coordinates of the particles. Therefore, the coefficients of their Jacobian matrix are constants or linear in the rectangular Cartesian coordinates. Where as in the formulation based on the relative coordinates, the constraint equations are derived based on loop closure equations which have the disadvantage that they do not directly determine the positions of the links and points of interest which makes the establishment of the dynamic problem more difficult. Also, the resulting constraint equations are highly nonlinear and contain complex circular functions. The absence of these circular functions in the point coordinate formulation leads to faster convergence and better accuracy. Furthermore, preprocessing the mechanism by the topological graph theory is not necessary as it would be the case with loop constraints.

Also, in comparison with the absolute coordinates formulation, the manual work of the local axes attachment and local coordinates evaluation as well as the use of the rotational variables and the rotation matrices in the absolute coordinate formulation are not required in the point coordinate formulation. This leads to fully computerized analysis and accounts for a reduction in computational time and memory storage. In addition to that, the constraint equations take much simpler forms as compared with the absolute coordinates.

The main kinematical properties of the suspension are described by the coordinates of the wheel centre point and the kingpin angle α and camber angle β (Adler, U.). The wheel centre point (point 11, see Fig. 3) is defined as the point at which the wheel spin axis intersects the wheel plane. Points 8 and 11 define the wheel spin axis. The coordinates of the wheel centre point can easily be determined by specifying its position relative to three other points located on the knuckle. Kingpin angle determines the steering aligning torque in conjunction with steering offset and wheel caster. The kingpin angle α is defined as the inclination angle of a fixed line on the knuckle (connecting points 6 and 8) relative to the vertical longitudinal plane, measured in the transverse plane of the vehicle (Adler, U.) and therefore from Fig. 3;

$$\alpha=\tan^{-1}\frac{y_8-y_6}{z_8-z_6}$$

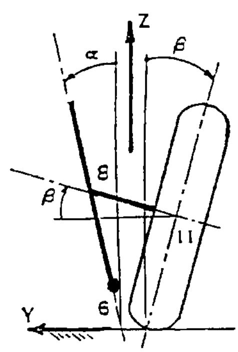

Fig. 3 Kingpin and camber angles

A positive angle α signifies a displacement of point 6 in the negative y direction. The camber angle β is the inclination of the wheel plane relative to the longitudinal vehicle plane, measured in the transverse plane of the vehicle and therefore ;

$$\beta=\tan^{-1}\frac{-(z_8-z_{11})}{(y_8-y_{11})}$$

Positive camber means that the wheels are tilted out at the top rather than at the bottom.

2.2 Velocity and acceleration analyses

The velocity equations are derived by differentiating Eq. (1) with respect to time and take the form

$$[C_q]\dot{\mathbf{q}}=0 \tag{2}$$

Since the velocity equations are linear, the vector of velocities ; $\dot{\mathbf{q}}=[\dot{q}_1, \dot{q}_2, \cdots, \dot{q}_{30}, \dot{\theta}]^T$ can be partitioned as ; $\dot{\mathbf{q}}=[\dot{u}^T, \dot{w}^T]^T$, and the velocity equation is written in the partitioned matrix form,

$$[C_6]\dot{\mathbf{u}}=[C_w]\dot{\mathbf{w}} \tag{3}$$

where $\dot{\mathbf{u}}=[\dot{x}_6, \dot{y}_6, \dot{z}_6, \cdots, \dot{z}_{10}]^T$ and $\dot{\mathbf{w}}=[\dot{x}_1, \dot{y}_1, \dot{z}_1, \cdots, \dot{z}_5, \dot{\theta}]^T$ are the unknown and known vectors of velocities, respectively and are given by,

$$[C_u]=\left[\begin{array}{ccccccccccccccc}
2x_{6,1} & 2y_{6,1} & 2z_{6,1} & 0 & 0 & 0 & 0 & 0 & 0 & 0 & 0 & 0 & 0 & 0 & 0 \\
0 & 0 & 0 & 2x_{7,2} & 2y_{7,2} & 2z_{7,2} & 0 & 0 & 0 & 0 & 0 & 0 & 0 & 0 & 0 \\
0 & 0 & 0 & 0 & 0 & 0 & 2x_{8,3} & 2y_{8,3} & 2z_{8,3} & 0 & 0 & 0 & 0 & 0 & 0 \\
0 & 0 & 0 & 0 & 0 & 0 & 0 & 0 & 0 & 2x_{9,4} & 2y_{9,4} & 2z_{9,4} & 0 & 0 & 0 \\
0 & 0 & 0 & 0 & 0 & 0 & 0 & 0 & 0 & 0 & 0 & 0 & 2x_{10,5} & 2y_{10,5} & 2z_{10,5} \\
2x_{6,7} & 2y_{6,7} & 2z_{6,7} & 2x_{7,6} & 2y_{7,6} & 2z_{7,6} & 0 & 0 & 0 & 0 & 0 & 0 & 0 & 0 & 0 \\
2x_{6,8} & 2y_{6,8} & 2z_{6,8} & 0 & 0 & 0 & 2x_{8,6} & 2y_{8,6} & 2z_{8,6} & 0 & 0 & 0 & 0 & 0 & 0 \\
2x_{6,9} & 2y_{6,9} & 2z_{6,9} & 0 & 0 & 0 & 0 & 0 & 0 & 2x_{9,6} & 2y_{9,6} & 2z_{9,6} & 0 & 0 & 0 \\
2x_{6,10} & 2y_{6,10} & 2z_{6,10} & 0 & 0 & 0 & 0 & 0 & 0 & 0 & 0 & 0 & 2x_{10,6} & 2y_{10,6} & 2z_{10,6} \\
0 & 0 & 0 & 2x_{7,8} & 2y_{7,8} & 2z_{7,8} & 2x_{8,7} & 2y_{8,7} & 2z_{8,7} & 0 & 0 & 0 & 0 & 0 & 0 \\
0 & 0 & 0 & 2x_{7,9} & 2y_{7,9} & 2z_{7,9} & 0 & 0 & 0 & 2x_{9,7} & 2y_{9,7} & 2z_{9,7} & 0 & 0 & 0 \\
0 & 0 & 0 & 2x_{7,10} & 2y_{7,10} & 2z_{7,10} & 0 & 0 & 0 & 0 & 0 & 0 & 2x_{10,7} & 2y_{10,7} & 2z_{10,7} \\
0 & 0 & 0 & 0 & 0 & 0 & 2x_{8,9} & 2y_{8,9} & 2z_{8,9} & 2x_{9,8} & 2y_{9,8} & 2z_{9,8} & 0 & 0 & 0 \\
0 & 0 & 0 & 0 & 0 & 0 & 2x_{8,10} & 2y_{8,10} & 2z_{8,10} & 0 & 0 & 0 & 2x_{10,8} & 2y_{10,8} & 2z_{10,8} \\
0 & 0 & 0 & 0 & 0 & 0 & 0 & 0 & 0 & 0 & 0 & 0 & 0 & 0 & 0
\end{array}\right] \tag{4}$$

and

$$[C_w]=\left[\begin{array}{cccccccccccccccc}
2x_{6,1} & 2y_{6,1} & 2z_{6,1} & 0 & 0 & 0 & 0 & 0 & 0 & 0 & 0 & 0 & 0 & 0 & 0 & 0 \\
0 & 0 & 0 & 2x_{7,2} & 2y_{7,2} & 2z_{7,2} & 0 & 0 & 0 & 0 & 0 & 0 & 0 & 0 & 0 & 0 \\
0 & 0 & 0 & 0 & 0 & 0 & 2x_{8,3} & 2y_{8,3} & 2z_{8,3} & 0 & 0 & 0 & 0 & 0 & 0 & 0 \\
0 & 0 & 0 & 0 & 0 & 0 & 0 & 0 & 0 & 2x_{9,4} & 2y_{9,4} & 2z_{9,4} & 0 & 0 & 0 & 0 \\
0 & 0 & 0 & 0 & 0 & 0 & 0 & 0 & 0 & 0 & 0 & 0 & 2x_{10,8} & 2y_{10,8} & 2z_{10,8} & 0 \\
0 & 0 & 0 & 0 & 0 & 0 & 0 & 0 & 0 & 0 & 0 & 0 & 0 & 0 & 0 & 0 \\
0 & 0 & 0 & 0 & 0 & 0 & 0 & 0 & 0 & 0 & 0 & 0 & 0 & 0 & 0 & 0 \\
0 & 0 & 0 & 0 & 0 & 0 & 0 & 0 & 0 & 0 & 0 & 0 & 0 & 0 & 0 & 0 \\
0 & 0 & 0 & 0 & 0 & 0 & 0 & 0 & 0 & 0 & 0 & 0 & 0 & 0 & 0 & 0 \\
0 & 0 & 0 & 0 & 0 & 0 & 0 & 0 & 0 & 0 & 0 & 0 & 0 & 0 & 0 & 0 \\
0 & 0 & 0 & 0 & 0 & 0 & 0 & 0 & 0 & 0 & 0 & 0 & 0 & 0 & 0 & 0 \\
0 & 0 & 0 & 0 & 0 & 0 & 0 & 0 & 0 & 0 & 0 & 0 & 0 & 0 & 0 & 0 \\
0 & 0 & 0 & 0 & 0 & 0 & 0 & 0 & 0 & 0 & 0 & 0 & 0 & 0 & 0 & 0 \\
0 & 0 & 0 & 0 & 0 & 0 & 0 & 0 & 0 & 0 & 0 & 0 & 0 & 0 & 0 & 0 \\
0 & 0 & 0 & 0 & 0 & 0 & 0 & 0 & 0 & 0 & 0 & 0 & 0 & 0 & 0 & -d_{6,1}\sin(\theta)
\end{array}\right] \tag{5}$$

Similarly, the acceleration equation is derived by differentiating the velocity Eq. (2) with respect to time as follows,

$$[C_q]\ddot{\mathbf{q}}+([C_q]\dot{\mathbf{q}})_q\dot{\mathbf{q}}=0 \tag{6}$$

Partitioning the vector of accelerations $\ddot{\mathbf{q}}$ into $[\ddot{\mathbf{u}}^T, \ddot{\mathbf{w}}^T]$ where $\ddot{\mathbf{u}}$ and $\ddot{\mathbf{w}}$ are the vectors of unknown and known accelerations respectively, the acceleration equation is expressed as,

$$[C_u]\ddot{\mathbf{u}}=[C_w]\ddot{\mathbf{w}}-([C_q]\dot{\mathbf{q}})_q\dot{\mathbf{q}}=0 \tag{7}$$

where the two submatrices $[C_u]$ and $[C_w]$ are defined by Eqs. (4) and (5) respectively and the square velocity term $([C_q]\dot{\mathbf{q}})_q\dot{\mathbf{q}}$ is expressed as follows,

$$[\dot{C}_q]\dot{\mathbf{q}}=\begin{bmatrix} 2\dot{x}_{6,1}^2+2\dot{y}_{6,1}^2+2\dot{z}_{6,1}^2 \\ 2\dot{x}_{7,2}^2+2\dot{y}_{7,2}^2+2\dot{z}_{7,2}^2 \\ 2\dot{x}_{8,3}^2+2\dot{y}_{8,3}^2+2\dot{z}_{8,3}^2 \\ 2\dot{x}_{9,4}^2+2\dot{y}_{9,4}^2+2\dot{z}_{9,4}^2 \\ 2\dot{x}_{10,5}^2+2\dot{y}_{10,5}^2+2\dot{z}_{10,5}^2 \\ 2\dot{x}_{6,7}^2+2\dot{y}_{6,7}^2+2\dot{z}_{6,7}^2 \\ 2\dot{x}_{6,8}^2+2\dot{y}_{6,8}^2+2\dot{z}_{6,8}^2 \\ 2\dot{x}_{6,9}^2+2\dot{y}_{6,9}^2+2\dot{z}_{6,9}^2 \\ 2\dot{x}_{6,10}^2+2\dot{y}_{6,10}^2+2\dot{z}_{6,10}^2 \\ 2\dot{x}_{7,8}^2+2\dot{y}_{7,8}^2+2\dot{z}_{7,8}^2 \\ 2\dot{x}_{7,9}^2+2\dot{y}_{7,9}^2+2\dot{z}_{7,9}^2 \\ 2\dot{x}_{7,10}^2+2\dot{y}_{7,10}^2+2\dot{z}_{7,10}^2 \\ 2\dot{x}_{8,9}^2+2\dot{y}_{8,9}^2+2\dot{z}_{8,9}^2 \\ 2\dot{x}_{8,10}^2+2\dot{y}_{8,10}^2+2\dot{z}_{8,10}^2 \\ d_{5,1}\cos(\theta)\,\dot{\theta}^2 \end{bmatrix} \tag{8}$$

Regardless of the order of nonlinearity of the constraint Eq. (1), the velocity and acceleration equations are linear in terms of $\dot{\mathbf{q}}$ and $\ddot{\mathbf{q}}$, respectively. If the position analysis has been formulated correctly, then the matrix $[C_u]$ is of a sufficient rank and becomes nonsingular. Therefore, the velocities and accelerations of the unknown points can be easily determined by solving both the linear Eqs. (3) and (7) using any numerical method. The velocities and accelerations of other points of interest can also be calculated if their positions are specified. The angular velocity and acceleration of any link in the mechanism, can be evaluated from the Cartesian coordinates, velocities, and accelerations of any three defined points on the link and are respectively given as,

$$\omega=\frac{\mathbf{v}_{j,i}x\mathbf{v}_{k,i}}{\mathbf{v}_{j,i}\cdot\mathbf{r}_{k,i}} \tag{9}$$

$$\alpha=\frac{\hat{\mathbf{a}}_{j,i}x\hat{\mathbf{a}}_{k,i}}{\hat{\mathbf{a}}_{j,i}\cdot\mathbf{r}_{k,i}} \tag{10}$$

where $\hat{\mathbf{a}}_{j,i}=\mathbf{a}_{j,i}-\omega x(\omega x\mathbf{r}_{j,i})$.

2.3 Results of the simulation

The chassis is assumed to be stationary and therefore the values of the velocities and accelerations of all known points (points 1, ⋯, 5) fixed on it are identically zero. The Cartesian coordinates of the known points are listed in Table 1. The driving variable θ is taken as function of time in the form, $\theta(t)=0.7+0.5t+0.125t^2$. The nonlinear equations of constraints (1) are solved by Newton-Raphson's method of successive approximation to determine the Cartesian coordinates of the unknown points for different time steps. Also, the Cartesian coordinates of the wheel centre (point 11) are estimated. Since the position analysis is a nonlinear problem which is solved by an iterative numerical method, it is expected that the problem of multiple solutions arrises. In order to avoid such problem, knowing the input driving variables, measurements can be used initially to obtain a good initial guess at the starting point of the position analysis. In the subsequent iterations, the problem of multiple solution can be overcome taking as a good initial guess the previous configuration of the system. The velocity and acceleration equations are solved using the L-U factorization with pivoting method. Table 2 presents some results of the kinematic analysis for two seconds of simulation as a result of changing the driver angle with time. Table 2 indicates also the initial guess for the coordinates of the unknown points. Table 3 presents the angular velocity and angular acceleration of the knuckle at various

Table 1 Cartesizn coordinates (m) of the known points

	Point 1	Point 2	Point 3	Point 4	Point 5
X	−1.396	−1.301	−1.0941	−0.9838	−1.095
Y	−0.025	0.1168	0.1987	0.2609	0.183
Z	−0.082	0.106	0.090	−0.0501	−0.0158

Table 2 Cartesian coordinates (m) of the unknown points

	Time (sec.)	0.00	0.25	0.50	0.75	1.00	1.25	1.50	1.75	1.95	Initial guess
Point	θ	40.1	47.72	56.22	65.62	75.92	87.11	99.19	112.17	123.20	
6	X	−1.196	−1.231	−1.261	−1.292	−1.315	−1.324	−1.316	−1.284	−1.223	−1.309
	Y	−0.181	0.261	0.320	0.367	0.400	0.415	0.408	0.372	0.305	0.412
	Z	0.259	0.218	0.166	0.102	0.027	−0.059	−0.153	−0.250	−0.326	−0.086
7	X	−1.114	−1.158	−1.212	−1.262	−1.302	−1.327	−1.336	−1.319	−1.267	−1.225
	Y	−0.013	0.126	0245	0.330	0.383	0.410	0.409	0.377	0.313	0.405
	Z	0.299	0.368	0.361	0.311	0.240	0.155	0.060	−0.039	−0.116	0.111
8	X	−1.107	−1.144	−1.193	−1.238	−1.270	−1.287	−1.285	−1.255	−1.190	−1.164
	Y	−0.010	−0.084	−0.183	0.263	0.315	0.345	0.350	0.332	0.299	0.435
	Z	0.221	0.303	0.316	0.281	0.218	0.140	0.051	−0.042	−0.114	0.070
9	X	−1.205	−1.232	−1.256	−1.278	−1.292	−1.290	−1.268	−1.215	−1.130	−1.231
	Y	0.183	0.206	0.240	0.279	0.309	0.325	0.34	0.302	0.271	0.532
	Z	0.161	1.136	0.108	0.060	−0.005	−0.084	−0.172	−0.261	−0.329	−0.145
10	X	−1.028	−1.067	−1.109	−1.153	−1.188	−1.212	−1.223	−1.219	−1.209	−1.137
	Y	0.094	0.202	0.290	0.364	0.418	0.453	0.467	0.458	0.424	0.489
	Z	0.276	0.294	0.277	0.232	0.167	0.089	0.001	−0.094	−0.178	−0.058

Table 3 Angular velocity (rad/s) and acceleration (rad/s^2) of the knuckle

Time (sec.)	0.00	0.25	0.50	0.75	1.00	1.25	1.5	1.75	1.95
ω_x	−3.47	−1.83	−1.02	−0.51	−0.27	−0.17	−0.15	−0.27	−1.14
ω_y	−0.36	−0.43	−0.47	−0.38	−0.32	−0.30	−0.30	−0.27	0.33
ω_z	0.43	−0.17	0.01	0.22	0.34	0.48	0.74	1.35	4.46
α_x	18.7	3.55	2.78	1.37	0.62	0.24	−0.11	−1.07	−20.8
α_y	1.41	−0.61	0.27	0.35	0.12	0.01	0.02	0.36	20.6
α_z	−7.74	−0.21	1.09	0.58	0.48	0.74	1.43	4.19	77.6

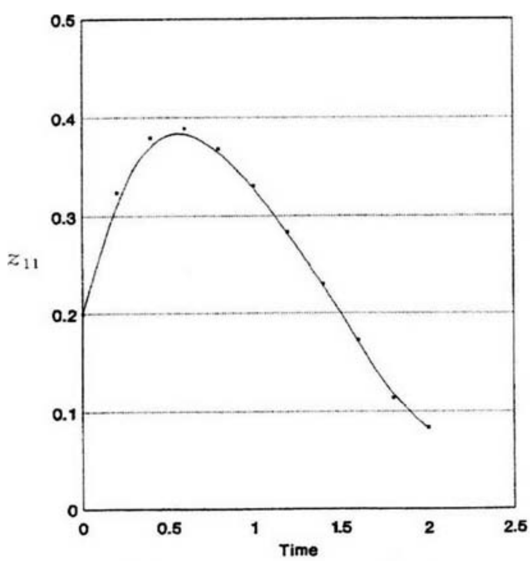

Fig. 4 Time (s) variation of z_{11} (m)

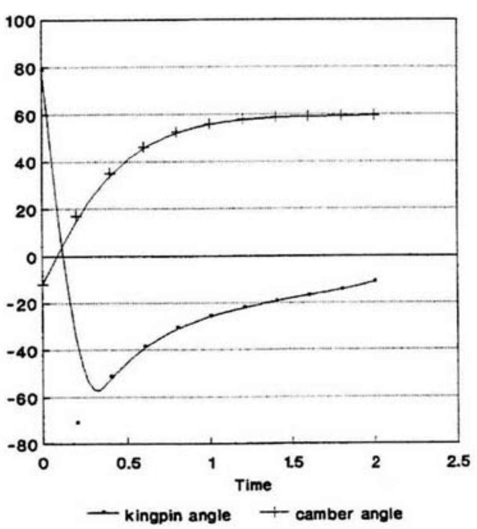

Fig. 5 Time (s) variation of the kingpin and camber angles (Deg)

time levels. Figure 4 presents the time variation of the z-coordinate of the wheel centre. Figure 5 shows the variation of the kingpin angle * and the camber angle * with time. It should be noted that the results of the simulation are tested and compared with the simulation results based on the absolute coordinates. This comparison proves the validity of the proposed method.

3. Conclusions

In this paper, an efficient algorithm for the numerical kinematic analysis of the spatial motor-vehicle multi-link five-point suspension mechanism is presented. The kinematic analysis is carried out in terms of the rectangular Cartesian coordinates of some defined points in the links and at the kinematic joints. The suggested algorithm eliminates the need to write redundant constraints and allows solving a reduced system of equations. The algorithm can be used to solve the initial position as well as the finite displacement problems. The results of the analysis indicate the simplicity and generality of the proposed algorithm.

References

Adler, U., Automotive Handbook, Bosch, FDI-Verlag, Approved Edition Under Licence SAE, ISPN 089283-518-6.

Akhras, R. and Angeles, J., 1990, "Unconstrained Nonlinear Least-Square Optimization of Planar Linkages for Rigid-Body Guidance," *Mechanism and Machine Theory*, Vol. 25, pp. 97~118.

Attia, H. A., 1993, A computer-Oriented Dynamical Formulation with Applications to Multibody Systems, Ph. D. Dissertation, Department of Engineering Mathematics and Physics, Faculty of Engineering, Cairo University.

Denavit, J. and Hartenberg, R. S., 1955, "A Kinematic Notation for Lower-Pair Mechanisms Based on Matrices," *ASME Journal of Applied Mechanics*, pp. 215~221.

Garcia de Jalon, J., Serna, M. A. and Aviles, R., 1981, "Computer Method for Kinematic Analysis of Lower-Pair Mechanisms-I Velocities and Accelerations," *Mechanism and Machine Theory*, Vol. 16, pp. 543~556.

Garcia de Jalon, J., Serna, M. A. and Aviles, R., 1981, "Computer Method for Kinematic Analysis of Lower-Pair Mechanisms-II Position Problems," *Mechanism and Machine Theory*, Vol. 16, pp. 557~566.

Garcia de Jalon, J. et al., 1982, "Simple Numerical Method for the Kinematic Analysis of Spatial Mechanisms," *ASME Journal on Mechanical Design*, Vol. 104, pp. 78~82.

Molian, S., 1968, "Solution of Kinematics Equations by Newton's Method," *Journal of Mechanical Engineering Science*, Vol. 10, No. 4, pp. 360~362.

Nikravesh, P. E., 1988, *Computer-Aided Analysis of Mechanical Systems*, Prentice-Hall.

Paul, B. and Krajcinovic, D., 1970, "Computer Analysis of Machines with Planar Motion-1. Kinematics, 2. Dynamics," *ASME Journal of Applied Mechanics*, Vol. 37, pp. 697~712.

Vilallonga, G., Unda, J. and Garcia de Jalon, J., 1984, "Numerical Kinematic Analysis of Three-Dimensional Mechanisms Using a 'Natural' System of Lagrangian Coordinates," *ASME Paper* No. 84-DET-199.

Wehage, R. A. and Haug, E. J., 1982, "Generalized Coordinate Partitioning of Dimension Reduction, in Analysis of Constrained Dynamic Systems," *ASME Journal of Applied Mechanical Design*, Vol. 104, pp. 247~255.